12th Multiphase Flow Conference
November 25-27 2014 Dresden

Granular flow and thermal performance of Moving Bed Heat Exchangers:
Comparison of the Euler-Euler model with experimental results

Torsten Baumann

DLR

Thermal Energy Storage (TES) for CSP-Plants

- **C**oncentrating **S**olar **P**ower (CSP) plants:
  - electricity from concentrated solar radiation
- Thermal energy storage:
  - Load following electricity production, dispatchability of CSP-system
  - based on **flowable particulates**: allows cost-effective large-scale solutions, simultanous use as storage material **and** HTF

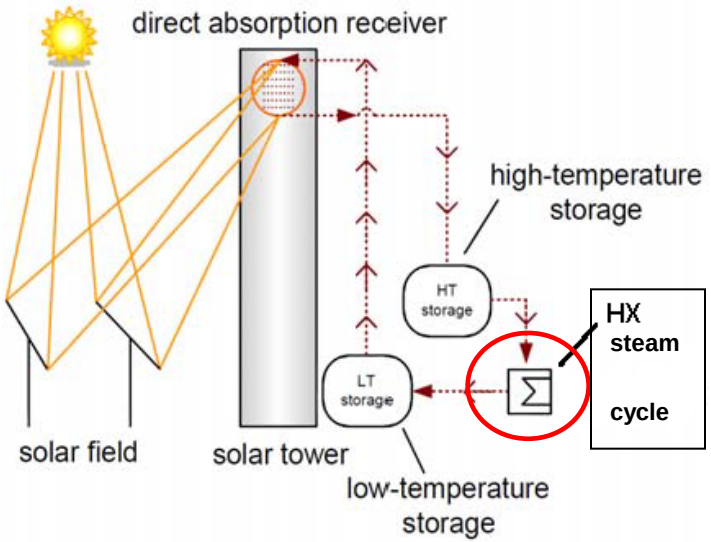

Heat exchanger for discharge of granular bulk

Moving Bed Heat Exchanger

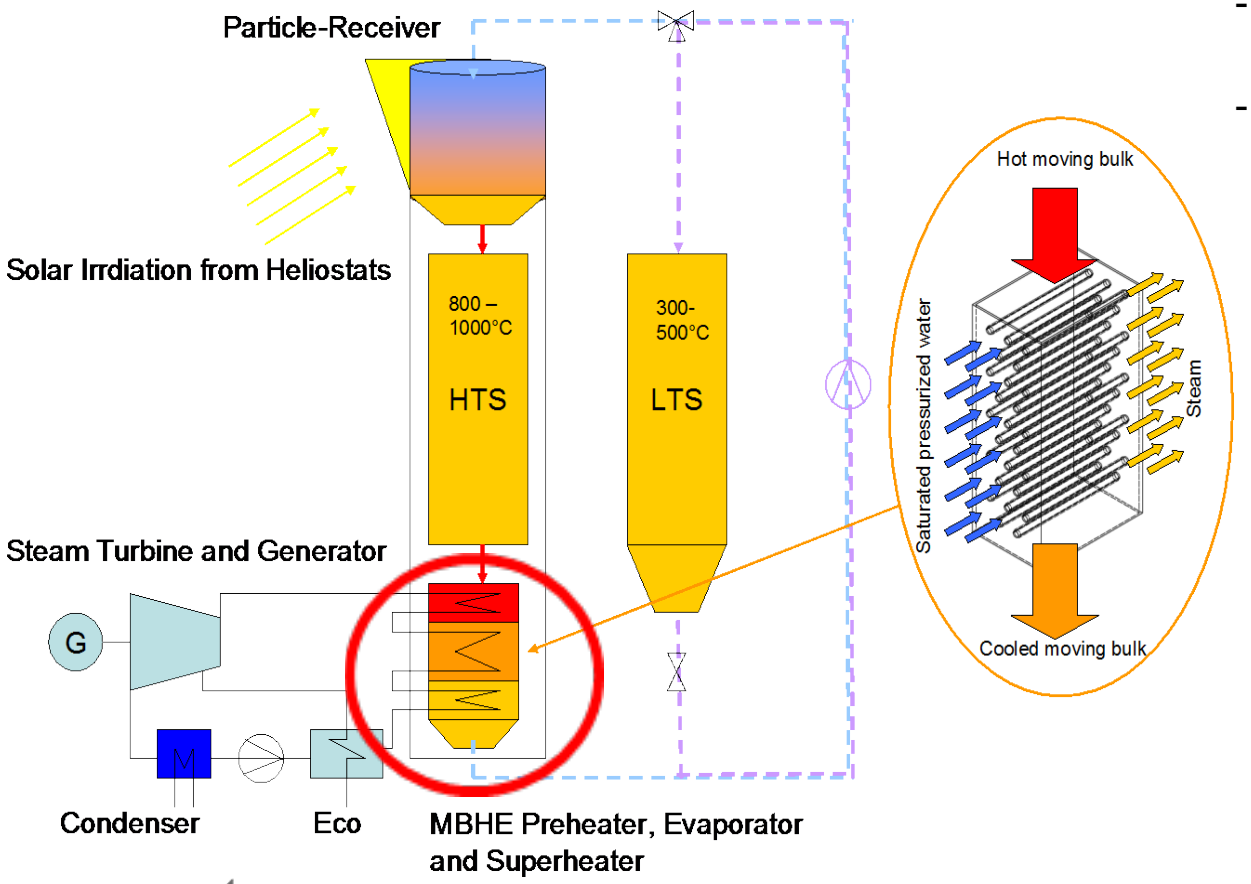

- Particles directly heated in Particle Receiver of CRS
- Storage itself is simple: Hot/cold storage containers
- But:
  - Discharge and supply of Rankine cycle ***requires a particle heat exchanger*** to run a Rankine or Bryton cycle
  - Not commercially available
  - In principle various technology options thinkable
  - **MBHE** promising
  - Design basis uncertain, with little flexibility

Challenges & Motivation

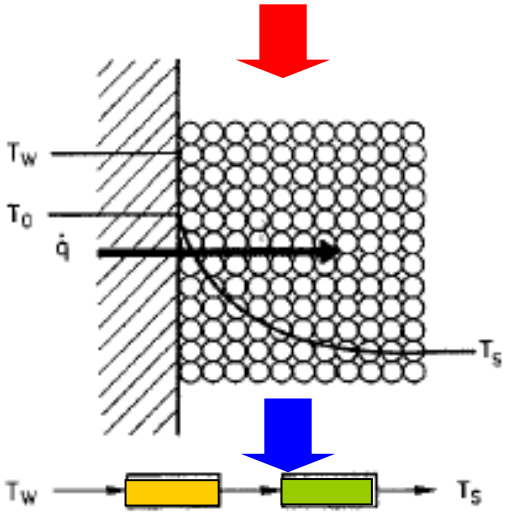

Overarching aim

Sizing of component and its system integration

- Quality of heat transfer, i.e. temperature loss?
- Required heat transfer area?
- Max. size and # of modules?

Problem

- Determination of thermal performance mandatory for MBHE-design
- Thermal performance of MBHE directly depends on velocity distribution of the bulk
- Flow behaviour of granular bulks differs from (Newtonian) fluids
  → **adequate determination of the flow field required**

$$h_{so} = \frac{2}{\sqrt{\pi}} \cdot \frac{\sqrt{(\rho \cdot c_p \cdot k)_{so}}}{\sqrt{t}}$$

Penetration theory proposed by Schlünder et al.

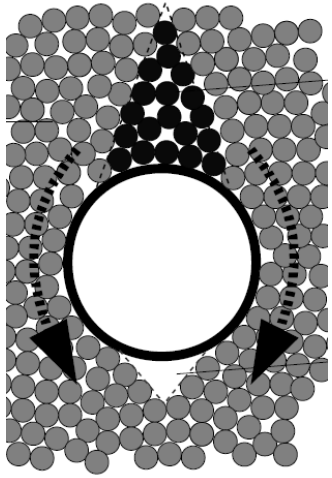

Proceeding

- **Euler-Euler** multiphase continuum approach to predict flow and heat transfer
- Parametric studies: tube shape, bundle arrangement
- Experimental validation of results

E.-U. Schlünder, E. Tsotsas. *Wärmeübertragung in Festbetten, durchmischten Schüttgütern und Wirbelschichten*. G. Thieme-Verlag, Stuttgart-New York, 1988

Model basis: Mass and momentum

- Euler-Euler multiphase continuum approach:
  - Considers both gaseous (air) and solid phase as interacting and penetrating continua
    → Navier Stokes conservation equations to be solved for each phase
  - Regards kinematic, collisional and frictional effects of solid phase

Phase volume fraction

Continuity: (both phases)

$$\frac{\partial}{\partial t}\left(\alpha_q \rho_q\right)+\nabla\cdot\left(\alpha_q \rho_q \vec{v}_q\right)=0$$

Interphase momentum exchange coefficient

Momentum: (gas)

$$\frac{\partial}{\partial t}\left(\alpha_f \rho_f \vec{v}_f\right)+\nabla\cdot\left(\alpha_f \rho_f \vec{v}_f \vec{v}_f\right)=-\alpha_f \nabla p+\nabla\cdot\bar{\bar{\tau}}_f+\alpha_f \rho_f \vec{g}+\alpha_f \rho_f\left(\vec{F}_f+\vec{F}_{lift,f}+\vec{F}_{vm,f}\right)+\sum_{p=1}^{n}\left(K_{fs}\left(\vec{v}_s-\vec{v}_f\right)+\dot{m}_{fs}\vec{v}_{fs}\right)$$

Momentum: (solid)

$$\frac{\partial}{\partial t}\left(\alpha_s \rho_s \vec{v}_s\right)+\nabla\cdot\left(\alpha_s \rho_s \vec{v}_s \vec{v}_s\right)=-\alpha_s \nabla p-\nabla p_s+\nabla\cdot\bar{\bar{\tau}}_s+\alpha_s \rho_s \vec{g}+\alpha_s \rho_s\left(\vec{F}_s+\vec{F}_{lift,s}+\vec{F}_{vm,s}\right)+\sum_{l=1}^{n}\left(K_{fs}\left(\vec{v}_f-\vec{v}_s\right)+\dot{m}_{fs}\vec{v}_{fs}\right)$$

Stress tensor (solid)

Stress tensor: (solid)

$$\bar{\bar{\tau}}_s=\alpha_s \mu_s\left(\nabla\vec{v}_s+\nabla\vec{v}_s^{T}\right)+\alpha_s\left(\lambda_s-\frac{2}{3}\mu_s\right)\nabla\cdot\vec{v}_s\bar{\bar{I}}$$

Shear viscosity: (solid)

$$\mu_s=\mu_{s,col}+\mu_{s,kin}+\mu_{s,fr}$$

Frictional viscosity: (solid)

$$\mu_{s,fr}=\frac{p_s \sin\phi}{2\sqrt{I_{2D}}}$$

Solid phase velocity field

Distribution of solid phase volume fraction

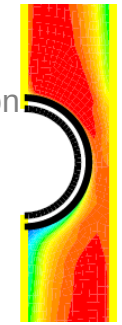

Model basis: Energy

- Euler-Euler multiphase continuum approach:
  - Considers both gaseous (air) and solid phase as interacting and penetrating continua
    → Navier Stokes conservation equations to be solved for each phase
  - Regards kinematic, collisional and frictional effects of solid phase

Phase volume fraction

Energy (both phases):
$$\frac{\partial}{\partial t}\left(\alpha_q \rho_q h_q\right) + \nabla \cdot \left(\alpha_q \rho_q \vec{u}_q h_q\right) = -\alpha_q \frac{\partial p_q}{\partial t} + \bar{\bar{\tau}}_q : \nabla \vec{u}_q - \nabla \cdot \vec{q}_q + S_q + \vec{Q}_{pq}$$

Heat transfer rate (interphase):
$$Q_{pq} = h_{pq}(T_p - T_q)$$

HT-coefficient (interphase):
$$h_{qp} = \frac{6 k_q \alpha_p \alpha_q Nu_p}{d_p{}^2}$$

Nusselt number via correlation (e.g. by Gunn)

Heat flux @ boundaries:
$$q = k_{SO}\left(\frac{\partial T}{\partial n}\right)_{wall}$$

Temperature contour

Modelling of the MBHE design:
Geometry study

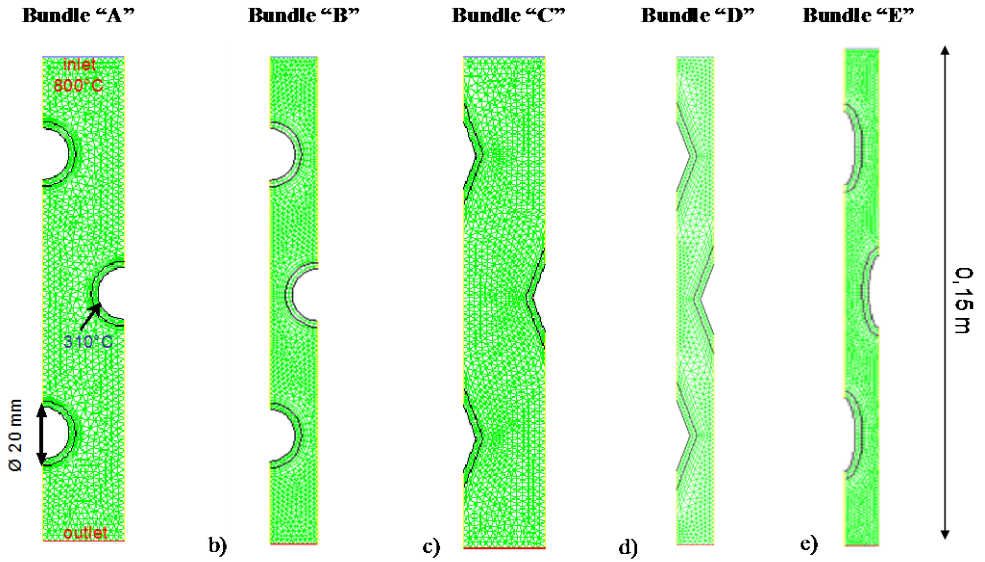

- Five MBHE-designs including three different tube shapes (circular, rhombic, oval)
- Varying staggered tube arrangement (different horizontal tube pitches)
- Minimal tube pitch (bundles B, D, E) and inclination angle (bundles C and D) determined from analysis of rheological bulk properties
- Sintered Bauxite is considered as bulk material; inlet velocity 2 mm/s

Material	Mean grain size [mm]	Molecular density [kg/m^3]	Molecular specific heat capacity [J/kgK]	Porosity of randomly packed bed [-]	Inner friction angle [°]	Restitution coefficient [-]
Sintered Bauxite	1.0	3900	1040	0.45	29.2	0.9

Results: Thermal performance

$$\bar{h} = \frac{q_{tube}}{(T_{\infty} - T_{tube})}$$

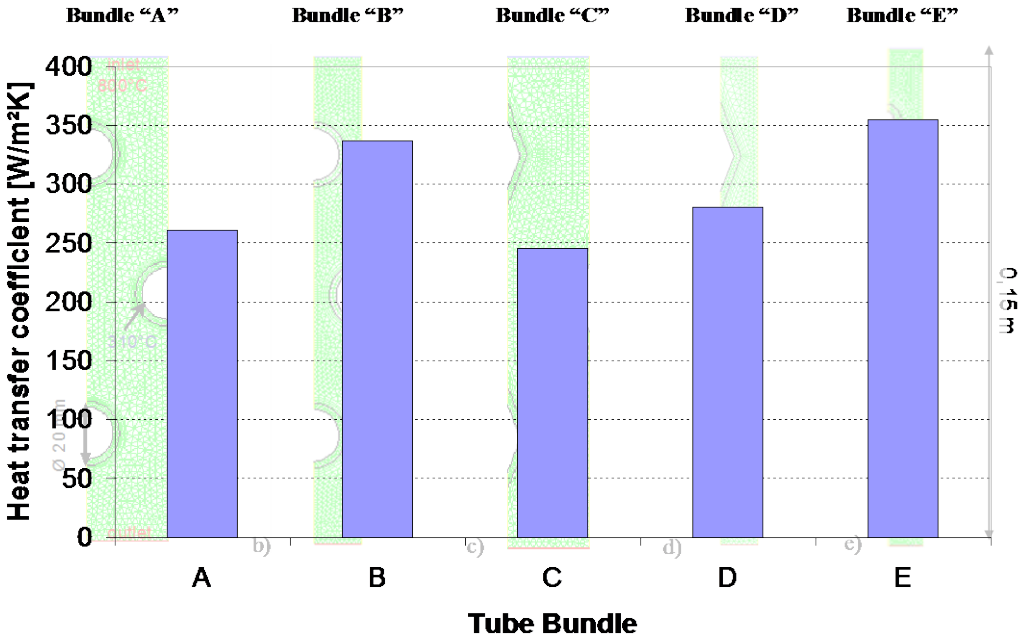

- High average heat transfer coefficients for narrow tube arrangements (B,D,E)
- No improvement of HTC by rhombic tubes
- Best heat transfer achieved for oval tubes

→ thermal performance is mainly affected by flow distribution of the bulk, which in return is influenced by the tube shape and bundle arrangement

Results: Velocity distribution

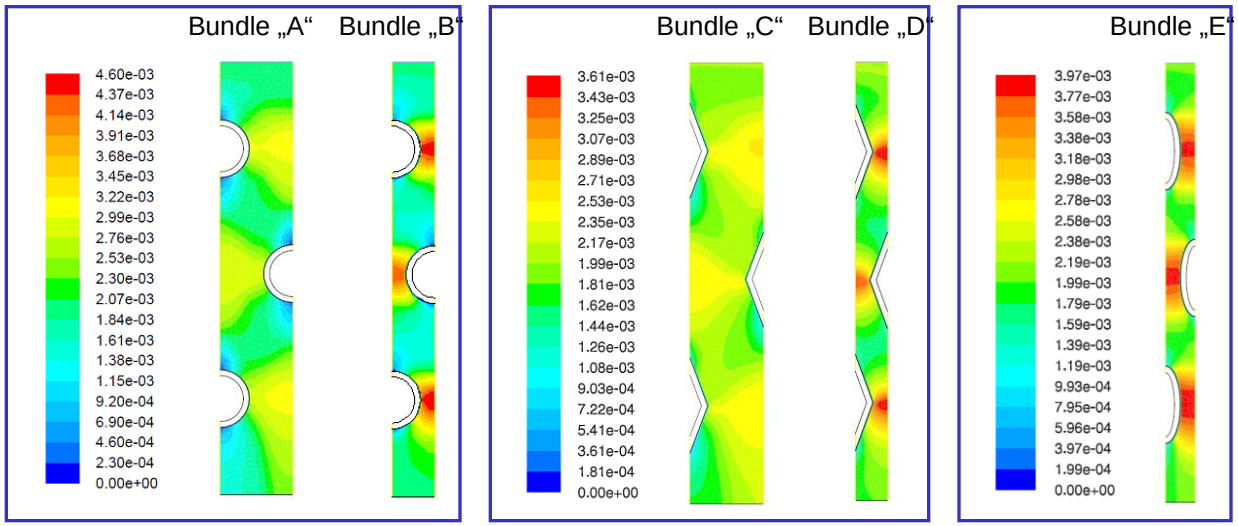

- Higher velocity in narrow bundle designs due to cross section constriction
- Formation of zones of low velocity (stagnant zones and voids) at circular tubes → low local surface velocity → insulating effect on heat transfer
- Rhombic design prevents formation of stagnant zones, but exhibits lower average surface velocity than circular tubes → higher contact time
- No emphasized formation of stagnant zones or voids at the oval shaped tubes, high share of high velocity along the surface → low contact time → high HTC

Results: Volume fraction distribution

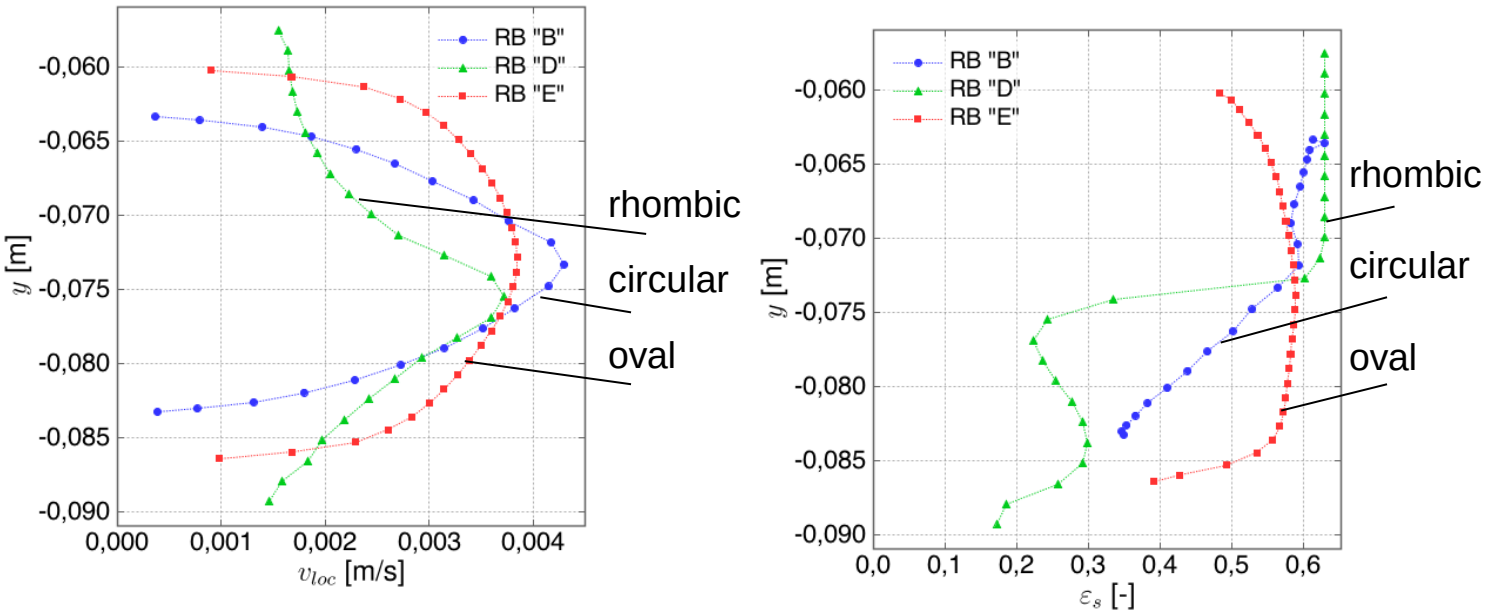

- High mean velocity for circular and oval tubes
- Solid volume fraction at circular tubes decreases close to the lower vertex
- Particles tend to detach from the lower half of the rhombic surface
- Integral solid packing at the oval tubes higher than for circular and rhombic tubes
- High void fraction leads a decreased integral heat transfer coefficient (heat transfer wall/air is lower than for wall/bulk)

Final HX design for optimized performance

Two different HX designs:

a.„Reference“ design, based on common 60°-triangle arrangement

b.„Adapted“ design, taking into account design parameters determined from analysis of rheological measurements → critical opening width = minimum distance between adjacent tube walls

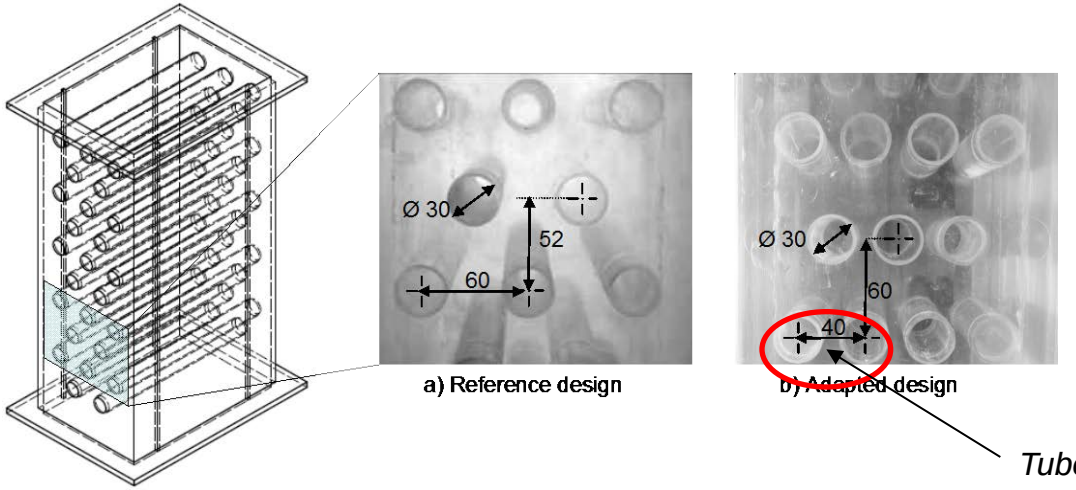

Acrylic glass models (for flow examination)

- Adapted design advantages:
  - High heat transfer rates due to high particle velocities at the tube wall
  - High HT-area to volume ratio → compact design

Example case: assumptions

Operating conditions & HX geometries

MBHE modules
- Cross-flow
- Gravity-driven bulk flow
- Staggered tube arrangement
- Tube diameter of 26.9 mm
- Adapted bundle :horizontal split ratio 1.37, based on analysis of rheological bulk properties

Bulk material
- Sintered bauxite and quartz sand
- Ø 0.5 ; 0.8 mm
- inner friction angle: 29°; 33°
- Restitution coefficient: 0.9

Operating conditions
- Bulk velocity @inlet: 1 – 5 mm/s
- Porosity @inlet: 0.48; 0.44

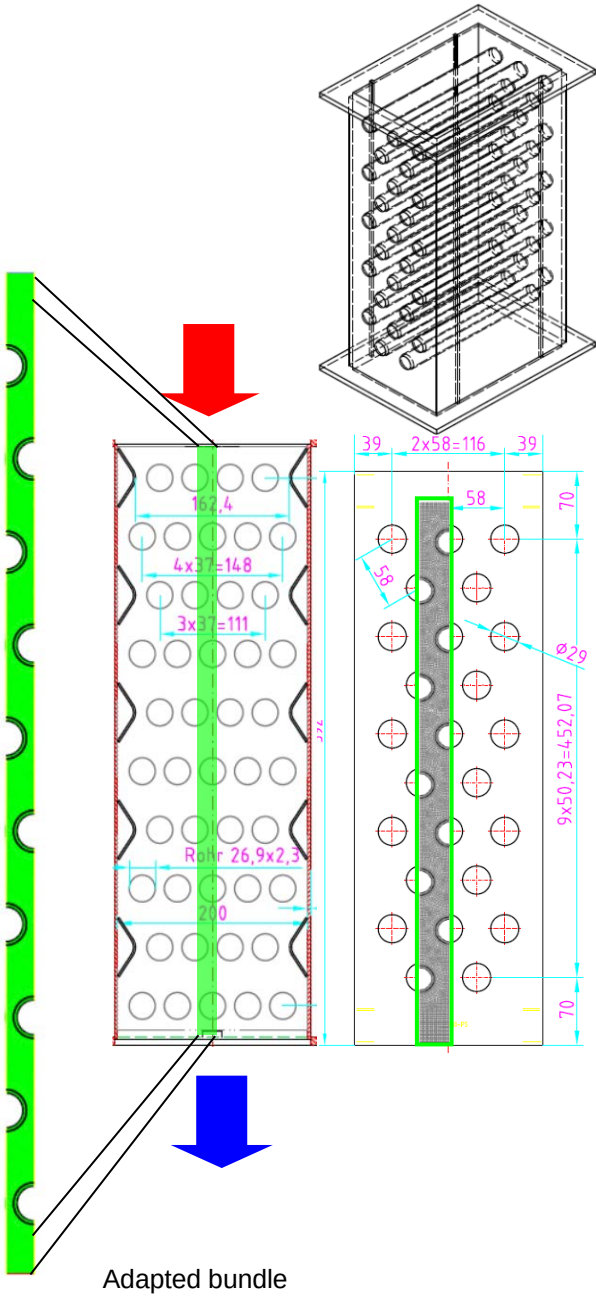

Adapted bundle

Experiments
Test Rig

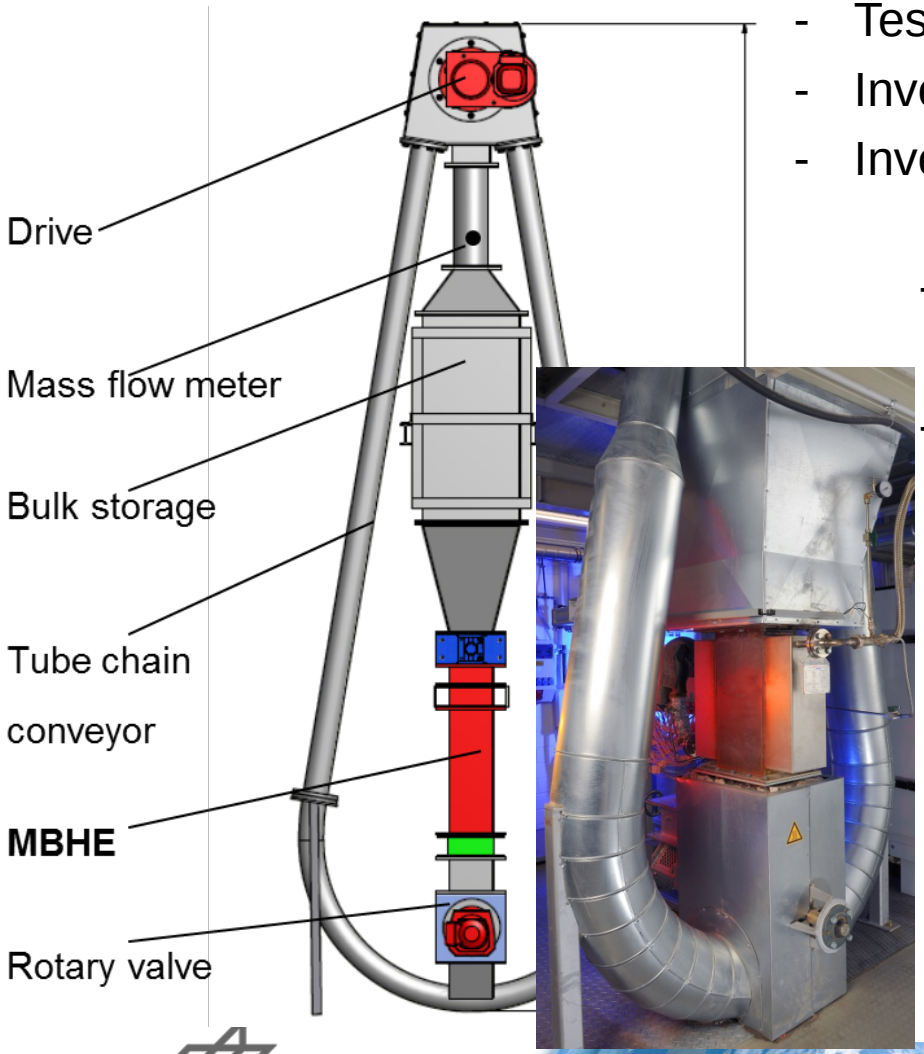

- Test bench allows integration of different MBHXs
- Investigation of granular flow field inside HX
- Investigation of thermal performance of HX

- Caloric heat determined applying temperatures of the granular core flow
- Outer heat transfer coefficient alpha computed in terms of overall heat transfer coefficient (NTU-method for crossflow HX)

Quick facts

Bulk loop	
Flow	0 - 1.0 m³/h
Heating power	35 kW
Inlet temperature	max. 600°C
Oil loop	
Flow	0 - 2.6 m³/h
Temperature	max. 300°C

Experiments
Flow Measurements - Setup & method

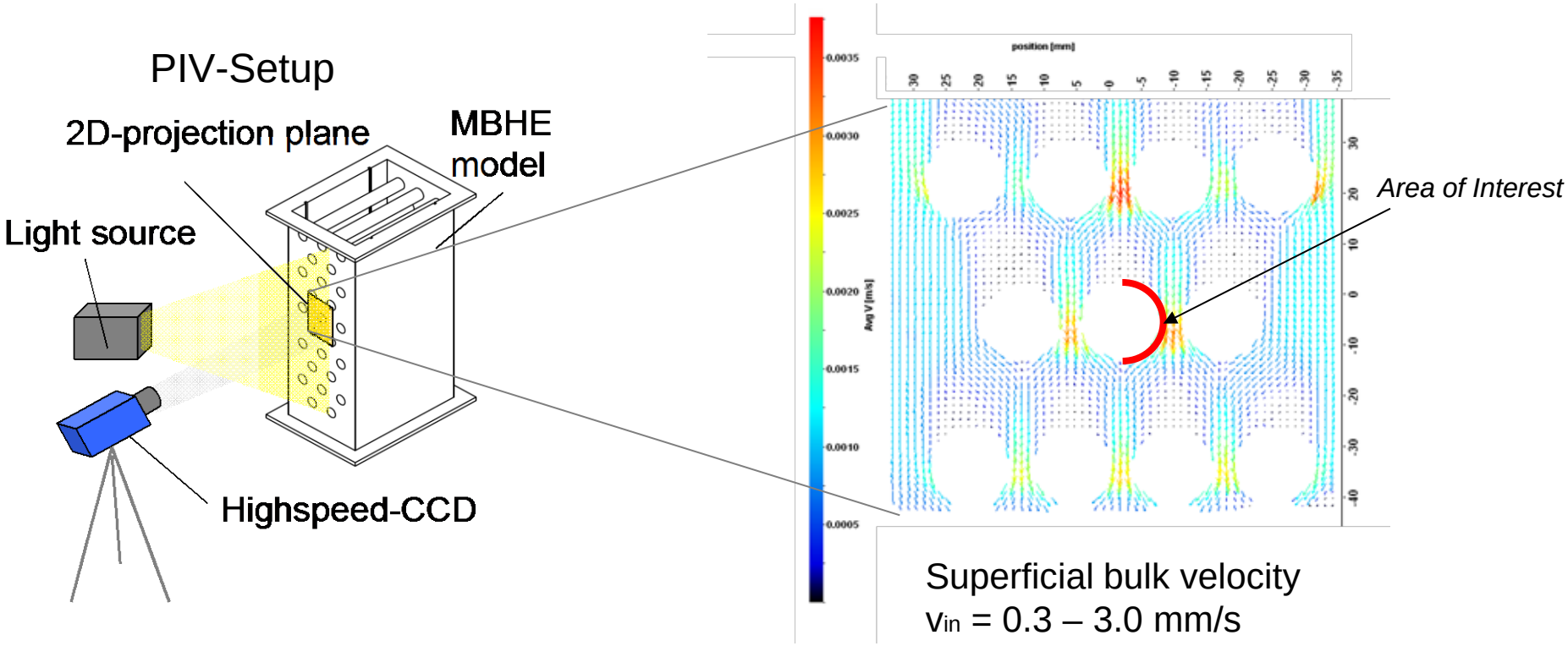

- Continuous mass flow inside the adapted tube bundle → no arching → appraised critical tube pitch suitable (same goes for the reference bundle)
- Equally distributed flow

Experiments

Flow Measurements - Results

Velocity profiles along tube walls (normalized)

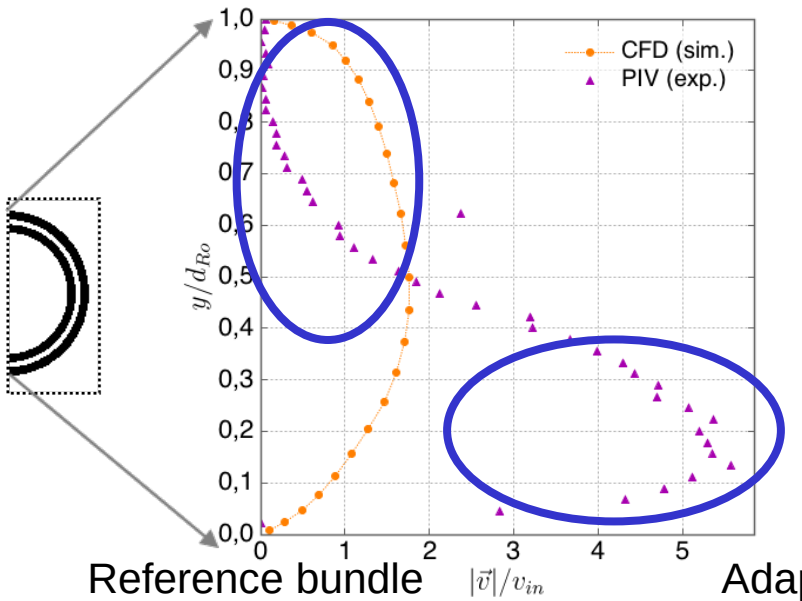

Reference bundle

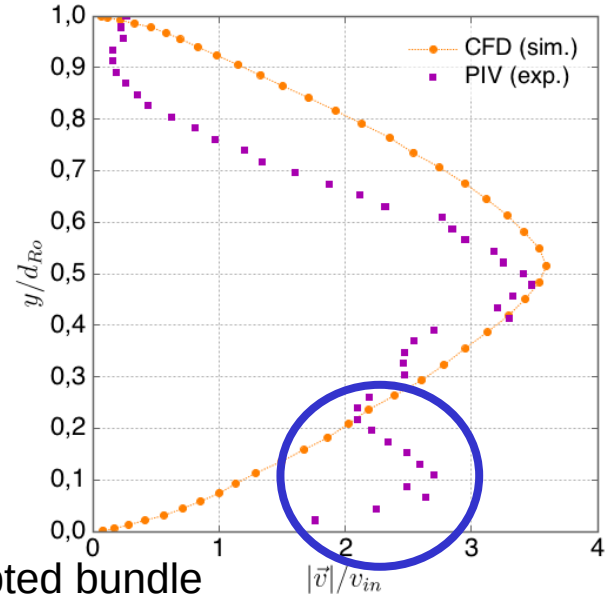

Adapted bundle

- Significant divergence (exp/sim)
- Exp: Much slower acceleration from upper vertex, max. velocity @ lower half
- Mean velocity up to 60% higher than in CFD

- Better consistence (exp/sim)
- Max velocity @ mid position
- Exp.: slight accelaration at lower half

→ Where do these effects come from?

Experiments
Flow Measurements - Results

Streamlines

Reference bundle

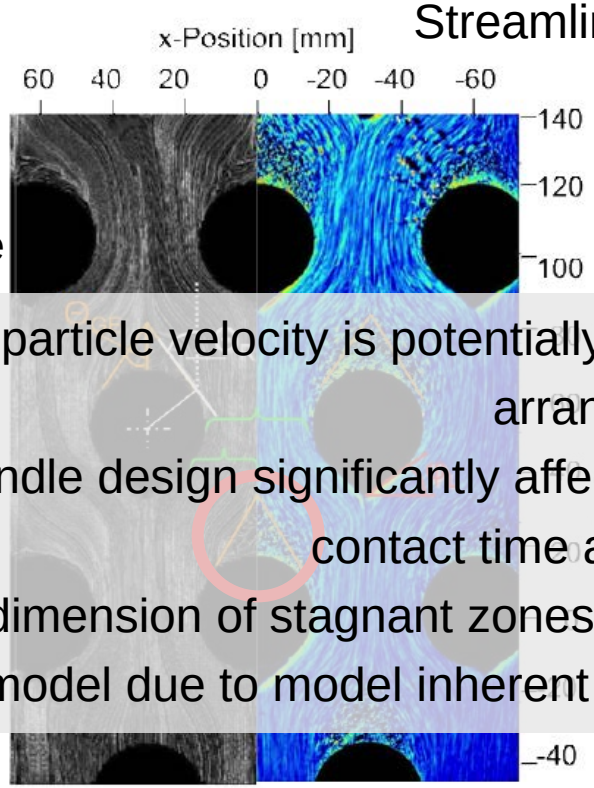

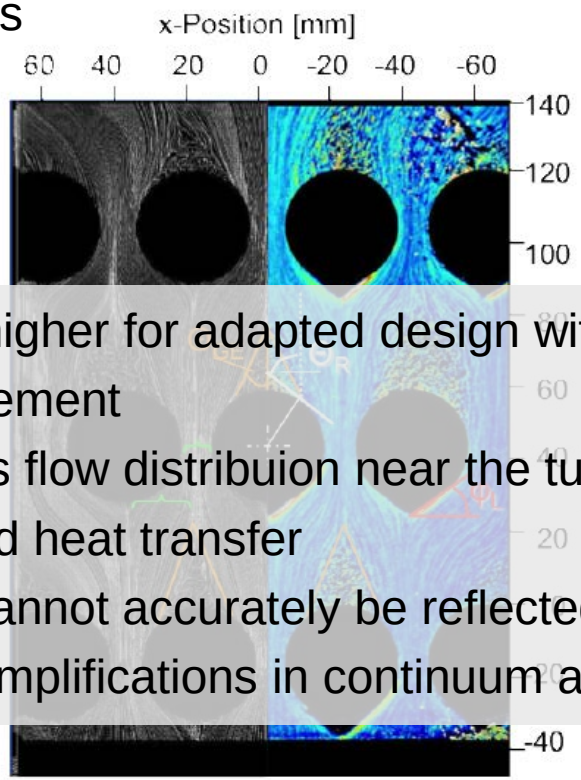

Adapted bundle

- Overall particle velocity is potentially higher for adapted design with narrow arrangement
- Tube bundle design significantly affects flow distribuion near the tube wall → contact time and heat transfer
- Specific dimension of stagnant zones cannot accurately be reflected by Euler-Euler model due to model inherent simplifications in continuum approach

- **Stagnant zones** constrict free cross section between upper, adjacent tubes in reference bundle → increased local velocity, spec. @ lower half
- Effect is minimized due to varied tube configuration in adapted bundle

Experiments
Thermal Characterization – Results

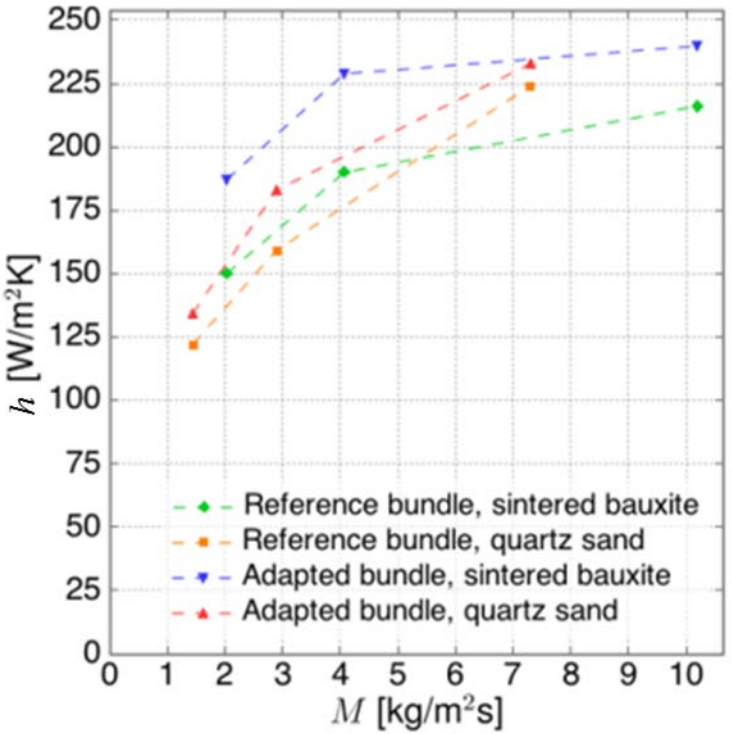

- Heat transfer regressively increases with mass flux
- Higher heat transfer coefficients for adapted tube bundle (up to 240 W/m²K)
- Slightly better performance for operation with sintered bauxite

Experiments
Thermal Characterization – Results

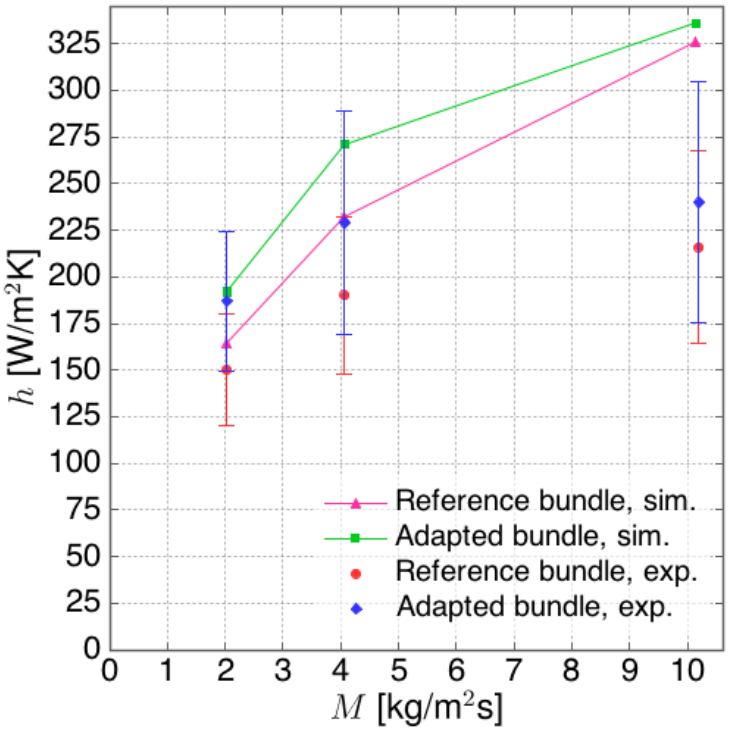

- Heat transfer regressively increases with mass flux
- Higher heat transfer coefficients for adapted tube bundle (up to 240 W/m²K)
- Slightly better performance for operation with sintered bauxite

- Increase of heat transfer coefficient lower than expected from CFD-results:
- Higher htc expected at higher mass fluxes according to penetration theory (approx. 300 W/m²K @ 10 kg/m²s, t_c = 5 s)

Experiments
Thermal Characterization – Results

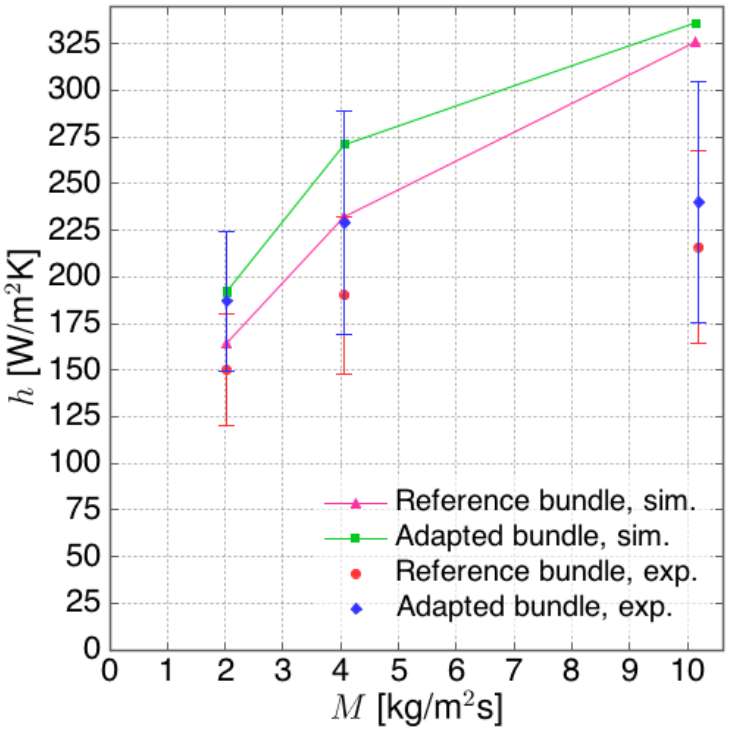

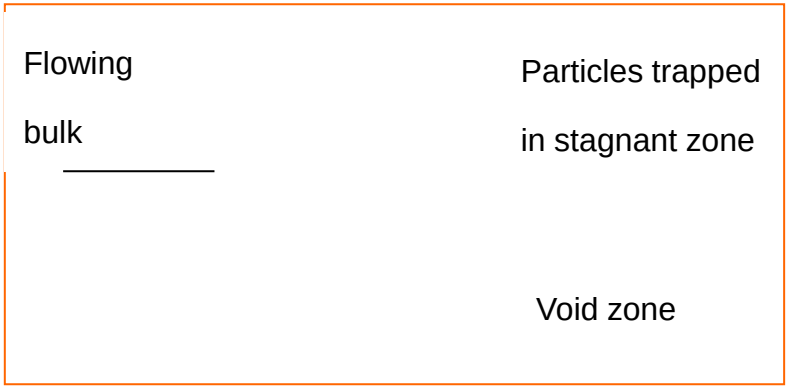

- Insulating effect of stagnant zone limits heat transfer at high massflux
- Effect less pronounce at lower mass fluxes since contact time is high either way

Summary & conclusions

- Narrow tube arrangement potentially increases thermal performance of MBHX
- Experimental flow visualisation analysis shows good agreement with the computed results
- Tube bundle configuration has significant influence on granular velocity distribution at tube walls, especially on stagnant zone formation
- Drawbacks in accuracy of flow due to model-inherent simplifications in granular rheology
- Despite insufficiency to accurately reflect discrete stagnant zones, the Euler-model is considered a solid basis for further MBHE parametric and design studies, specifically for moderate mass fluxes

Outlook:

- Identification and implementation of improved models for granular viscosity
- Validation and further design studies (Simulations and Experiments)

Torsten Baumann

Institute of Technical Thermodynamics/ Thermal Process Technology
German Aerospace Center
Pfaffenwaldring 38-40
70569 Stuttgart (Germany)

Phone:+49 (0)711 6862-432
E-mail: torsten.baumann@dlr.de